Journal of Catalysis **196,** 366–374 (2000)
doi:10.1006/jcat.2000.3036, available online at http://www.idealibrary.com on IDEAL®

Direct Production of Hydrogen Peroxide with Palladium Supported on Phosphate Viologen Phosphonate Catalysts

Venkatesan V. Krishnan, Alexandre G. Dokoutchaev, and Mark E. Thompson[1]

Department of Chemistry, University of Southern California, Los Angeles, California 90089-0744

Received May 30, 2000; revised August 7, 2000; accepted August 7, 2000

The optimization of porous hafnium phosphate viologen phosphonate (HfPOPV(*X*)) catalyst, [(HfF)$_2$(PO$_4$)(O$_3$PCH$_2$CH$_2$–4,4'-bipyridinium–CH$_2$CH$_2$PO$_3$)]F · 2H$_2$O with Pd–metal nanoaggregates, has been attempted. In addition to the development of a novel technique for making this catalyst by hydrothermal incorporation, an extensive optimization of the process conditions to make hydrogen peroxide from H$_2$ and O$_2$ has been carried out. The optimal reaction medium for this process was methanol in conjunction with sulfuric acid. Under atmospheric conditions, over 3.5 M H$_2$O$_2$ has been produced in 50 h. A technique has also been developed to measure the water formed from the undesirable H$_2$O$_2$ reduction step that occurs in series–parallel to the desired H$_2$O$_2$ production step. The selectivity toward the production of H$_2$O$_2$ in the case of the hydrothermally incorporated catalysts is over 70% under atmospheric conditions. The maximum rate of production of H$_2$O$_2$, achieved in anhydrous methanol–H$_2$SO$_4$ media and hydrothermally incorporated Pd–HfPOPV(*X*) is about 4.1 mmol/(g min). However, the rate measured here is probably that of external mass transfer (at the liquid–gas interface) because the resistance due to it is the rate-determining step.

Key Words: **hydrogen peroxide; direct production; heterogeneous catalyst; hydrothermal incorporation; viologen; palladium; kinetic study.**

INTRODUCTION

The commercial production of hydrogen peroxide has been an industrial challenge for the second half of this century. Hydrogen peroxide has gained significant commercial value recently as an environmentally friendly oxidant in industries such as paper and textiles. The best known process of producing H$_2$O$_2$ is the Reidl–Pfleiderer process, which was formulated during the second World War. The majority of the H$_2$O$_2$ produced globally is based upon this process (1). The Reidl–Pfleiderer process involves the use of a 2-alkylanthrahydroquinone catalyst. The anthraquinone is dissolved in a suitable hydrophobic solvent (called the working solution) and is hydrogenated in the presence of a heterogeneous catalyst. The working solution containing the resultant 2-alkylanthrahydroquinone is separated from the hydrogenation catalyst and treated with oxygen to regenerate the 2-alkylanthraquinone and form H$_2$O$_2$. The H$_2$O$_2$ is then removed from the working solution by aqueous extraction and concentrated to the desired level (1). The predominance enjoyed by this process comes from the fact that it is a safe method for reacting hydrogen and oxygen, a very explosive mixture. In this process, the oxygen and hydrogen are never contacted in a single medium, largely eliminating the prospect of explosion. However, this requires energy-intensive separation and concentration steps.

Many researchers have worked on developing a direct method that will produce H$_2$O$_2$ safely from mixtures of H$_2$ and O$_2$, minimizing separation costs. An added benefit of a direct process would be the ability to prepare H$_2$O$_2$ solutions at higher concentrations than those possible for the Reidl–Pfleiderer process, potentially eliminating the final concentration step in that process. Direct combination of hydrogen and oxygen to form H$_2$O$_2$ in aqueous media with supported metal catalysts has been the general theme of several patents. Notable among these efforts have been the production of H$_2$O$_2$ directly using Pt/Pd on silica catalysts by Gosser and co-workers (2–4) with a combination of phosphonate and an acid promoter in the reaction media to produce H$_2$O$_2$. The acid promoter in this system must be a hydrohalous acid (HCl or HBr) for the catalysis to be efficient. Kawakami *et al.* (5) have produced H$_2$O$_2$ directly in a two-phase system using a Group VIII metal catalyst and stabilizers. Chuang and Zhou (6) used Pd supported on a fluorinated graphite catalyst. The degree of fluorination of support is a critical parameter. Also, the presence of Cl$^-$ ions in the reaction media is very important in keeping the catalyst active. Dalton *et al.* (7) have used Pd on carbon catalysts and have developed a way to lengthen catalyst activity by the removal of undesirable salts of Pd formed by the interaction of the metal with the acidic liquid media. Meiers and co-workers have recently reported coupling a direct H$_2$O$_2$ catalyst (supported Pd) with a catalyst for olefin

---

[1] To whom correspondence should be addressed: Prof. Mark E. Thompson, LJS370, Department of Chemistry, University of Southern California, Los Angeles, CA 90089-0744. Fax: (213)740-8594. E-mail: met@usc.edu.

0021-9517/00 $35.00

epoxidation (titanium silicate) (8). The overall epoxidation yield for this system was good.

Our approach to the development of a catalyst for the direct production of H_2O_2 is to combine the use of an organic catalyst for the activation of O_2, due to the high potential selectivity of the organic species, with a metal catalyst for the activation of H_2. The organic group we chose for this catalyst is a viologen, i.e., *N*,*N*′-dialkyl-4,4′-bipyridinium. Viologen was chosen for two reasons. Farrington *et al.* (9) have shown that the rate of reaction of methylviologen with dissolved oxygen is very high, $k = 8 \times 10^8\ \mathrm{M}^{-1}\ \mathrm{s}^{-1}$. In addition to the high reaction rate for peroxide production, we have developed the synthesis of porous or zeolitic materials based on viologen building blocks (10). These materials are metal phosphate/phosphonate compounds (typically of Zr or Hf) and have been structurally characterized by powder X-ray diffraction studies (11). The porous structure gives the viologen-based catalyst a high surface area and gives us the ability to incorporate metal catalysts in intimate contact with the organic catalyst. The metal catalyst incorporated into the porous material is a noble metal (i.e., Pt or Pd), such that it will show good activity for the activation of hydrogen. Thus, the catalysis here corresponds to several steps, all carried at the metal–viologen catalyst interface, summarized in Eqs. [1a]–[1d]. Hydrogen is split into protons and electrons by the noble metal and the electrons transferred to the viologen groups (viol) (12). The reduced viologen then reacts with O_2 to give the desired product H_2O_2.

$$H_2 \rightarrow 2H^+ + 2e^- \qquad [1a]$$

$$2e^- + 2\mathrm{viol}^{2+} \rightarrow 2\mathrm{viol}^{+/\cdot} \qquad [1b]$$

$$2H^+ + O_2 + 2\mathrm{viol}^{+/\cdot} \rightarrow 2\mathrm{viol}^{2+} + H_2O_2 \qquad [1c]$$

$$\text{Net:}\quad H_2 + O_2 \rightarrow H_2O_2. \qquad [1d]$$

The undesirable reaction, i.e., $H_2O_2 + H_2 \rightarrow 2H_2O$, is also catalyzed by these materials, but it only competes with peroxide formation at higher concentrations of H_2O_2. As the concentration of H_2O_2 increases, the rate of peroxide reduction approaches the rate of H_2O_2 formation, and the concentration of H_2O_2 then remains fixed. The concentration of H_2O_2 at this stage is the steady-state concentration and is a direct measure of the efficiency of the catalyst.

Our initial work on this catalyst system (13) showed a dependence of hydrogen peroxide production on the presence of halide ions in the aqueous reaction media and suggested that a mixture of Pt and Pd in the catalyst was optimal. The incorporation of the Group VIII metal was accomplished by ion exchange of metal salts into the porous material and subsequent reduction with hydrogen to fine metal particles. The goal was to form the metal particles within the micropores of the catalyst. Unfortunately, in later work we found that this method of incorporation resulted in the deposition of large agglomerates of Pd and Pt on the surfaces of the porous viologen catalyst (14). Moreover, when $PtCl_4^{2-}$ and $PdCl_4^{2-}$ salts are used together, the metal particles formed upon reduction are completely segregated into isolated Pd and Pt particles. While small amounts of Pt (ca. $Pd_{95}Pt_5$) were found to increase the production of H_2O_2 in our initial study (13), we found in the later study that the best catalyst contains only Pd (14). To get the highest activity of our catalyst system, we have to decrease the amount of metal agglomeration on the surface of the particles and ensure higher dispersion of metal. Our work in improving the properties of this catalyst is described in this paper.

Aside from the catalyst itself, several factors could affect the rate of H_2O_2 buildup in the reactor, such as the external mass transfer resistances at the liquid–gas and liquid–solid interface, the solubility of the gases in the liquid media, and the pressure. The effect of some of these parameters have been investigated, and based upon their influence on the H_2O_2 production rate, the optimization of the catalyst and reaction media has been attempted in this work.

METHODS

Synthesis and characterization of catalysts. The synthesis of hafnium (or zirconium) phosphate viologen–phosphonates by a hydrothermal method has been described previously (11, 14). The hydrothermal incorporation technique used was based on this synthesis and is described below.

Hydrothermal synthesis. Teflon-lined bombs (PARR, 4744 General Purpose) with volumes of 20 or 45 ml were used for the hydrothermal synthesis. Reactant mixture A was prepared by dissolving either 2.28 mmol of $HfOCl_2 \cdot 8H_2O$ (or $ZrOCl_2 \cdot 8H_2O$) along with 0.073 ml (2.28 mmol) of 50% HF (stoichiometric amount) or 0.365 ml (5 times the stoichiometric amount) or 0.73 ml (10 times the stoichiometric amount), in 17 ml of water. Reactant mixture A was prepared directly in the bomb. Reactant mixture B contained 0.507 g (1.14 mmol) of $H_2O_3P(CH_2)_2$–viologen–$(CH_2)_2PO_3H_2 \cdot Cl_2$ ($\underline{\mathrm{PV}} \cdot Cl_2$) and 0.078 ml (1.14 mmol) of 85% H_3PO_4, along with 8.5 ml of water. An equal volume (8.5 ml) of aqueous solution of Na_2PdCl_4 (or K_2PdCl_4, 0.285 to 1.14 mmol) was slowly added to mixture B. Immediate precipitation was observed. Ultrasonication or fast stirring was used during mixing to obtain the finest precipitate particles. Reactant mixture B was then added slowly to A in the bomb. The bomb was sealed and placed in an oven kept at 125°C for a period of 5 days. The optimal crystallization time and temperature of the hydrothermal crystal growth were determined by trial and error. The amounts of all reagents used for a particular catalyst mentioned in this paper are summarized in Table 1.

TABLE 1

Reagent Concentrations and ICP-MS Elemental Analysis of Different Catalysts (% in Brackets Indicate Loading by Weight)

Catalyst	Volume H_2O, ml	[$HfOCl_2$], mM	[HF], mM	[PV], mM	[H_3PO_4], mM	[Na_2PdCl_4], mM	[P], mmol/g	[Pd], mmol/g	[Pd]/[P]
HT1-1	17	1.14	5.7	0.57	0.57	0.57	2.68	0.54 (5.7%)	0.2
HT1-2	17	1.14	11.4	0.57	0.57	0.57	2.66	0.64 (6.8%)	0.24
HT2	17	0.57	2.85	0.285	0.285	0.285	3.5	0.87 (9.2%)	0.25
HT3-1	34	1.14	5.7	0.57	0.57	0.57	1.67	0.46 (4.9%)	0.28
HT3-2	34	1.14	11.4	0.57	0.57	0.57	1.58	0.73 (7.7%)	0.46
IEx	34	2.28	11.4	1.14	1.14	No	2	1.08 (11.4%)	0.54

Note. The bottom line shows the composition of typical ion-exchanged catalysts. Numbers 1 or 2 after the dash in the catalyst name correspond to [HF]: 5 or 10 times [$HfOCl_2$].

Reduction. Reduction was carried out by bubbling hydrogen through an aqueous suspension of the ion-exchanged or hydrothermally synthesized material for 3 h at about 45–50°C, although the reduced metal forms even at room temperature.

Catalyst characterization. The elemental composition of the catalysts was carried out by inductively coupled plasma-mass spectrometry (ICP-MS, using Perkin-Elmer, Elan 5000 system). The structure of the crystals was determined by powder X-ray diffraction (Rigaku, Rotaflex RU-2a, using Cu $K\alpha$ radiation, with a 2Θ scan from 4° to 80°). These catalysts were also characterized by transmission electron microscopy (TEM, using Phillips EM420, voltage of 120 kV), primarily to determine the size and the dispersion of Pd particles.

Catalysis.

1. Pre-treatment of the catalyst prior to kinetic experiments: Part of the preparation of the catalyst included the reduction of the hydrothermally incorporated catalyst by bubbling a stream of pure H_2 through the slurry of catalyst in water, at room temperature. This reduces all MCl_4^{2-} to $M^{(0)}$ particles.

Prior to any experiment, the catalyst might still contain oxidized metal (PdO), if the catalyst is stored for an extended period. TEM micrographs showed Pd particles of 15–20 Å in freshly prepared catalyst, highly susceptible to aerobic oxidation. Prereduction of the catalyst slurry thus maximized the activity of the Pd sites and was done routinely. The prereduction did not affect the pH of the solution.

2. Production of H_2O_2: All reactions were carried out at room temperature, i.e., 20–23°C. Each reactor was a 50-ml centrifuge tube, charged with a slurry of catalyst in the appropriate reaction media, consisting of 25 mg of catalyst, 10 ml of 0.1 M aqueous mineral acid (H_2SO_4 or HCl), and 20 ml of a given organic solvent. Pure hydrogen and oxygen were then continuously bubbled through the slurry with 2-mm polyethylene tubing. The flow rate of hydrogen was 15 cc/min and that of oxygen was 200 cc/min. The oxygen stream was passed through a bubbler, containing the given organic solvent prior to entering the reactor, to prevent excessive evaporative loss of organic solvent from the reactor. Kinetic studies using 30 ml of methanol with 51 μl of concentrated sulfuric acid as the reaction medium (referred to as anhydrous conditions) have also been carried out. This medium has no more than 1% water (from commercial concentrated sulfuric acid).

3. Measurement of [H_2O_2]: The measurement of hydrogen peroxide concentration was carried out colorimetrically. A sample of the reaction medium (0.1 ml or less) was removed and diluted appropriately. The H_2O_2 in this sample reacts with a CHEMETRICS indicator (a mixture of ferrous ion and ammonium thiocyanate) to give a red solution with an absorbance maximum at 475 nm. The intensity of this peak can then be correlated with the concentration of H_2O_2 by Beer's law.

4. Estimation of selectivity for production of H_2O_2: A gas chromatograph, HP 5890, with a thermal conductivity detector was used for this purpose. The selectivity measurements were carried out only in the case of anhydrous media. The separation of water from the methanol media is effective, but a problem arises when the sample is injected into the column. The H_2O_2 present in the sample decomposes in the column, by autooxidation, to give water and oxygen. The degree of autooxidation evident in the GC trace varies with the H_2O_2 concentration. To measure water accurately, it is important to accurately account for the water produced by this autooxidation. A 0.2-ml sample from the reactor was treated with 1–2 mg of MnO_2, which rapidly and cleanly autooxidized H_2O_2 to water and oxygen. The total water measured by GC included the water formed during the reaction as well as that arising from the decomposition of H_2O_2 (from the MnO_2 treatment). Subtraction of water due to H_2O_2 (measured by colorimetric analysis) from the total water concentration measured by GC, gave the true concentration of water formed from H_2O_2 reduction.

The quantitative estimation of selectivity was calculated as follows:

$$\text{Selectivity (fraction)} = \text{rate, desired}/(\text{rate, desired} + \text{rate, undesired})$$

$$\text{selectivity} = \frac{r_1}{r_1 + r_2} = \frac{[H_2O_2]}{[H_2O_2] + [H_2O]/2}. \quad [2]$$

RESULTS

The crystal structure of the catalysts used here have been confirmed by powder XRD to be that of HfPOPV(X) [i.e., $Hf_2(PO_4)(O_3PCH_2CH_2\text{viologen}CH_2CH_2PO_3)F_3 \cdot 2H_2O$] (11). Two methods of metal incorporation were compared: ion exchange (11, 14) and newly developed hydrothermal incorporation. The main advantage of the latter method is the incorporation of metal ions prior to HfPOPV(X) structure formation. This was achieved through formation of a sparingly soluble complex between $H_2O_3PCH_2CH_2$ viologen$^{2+}CH_2CH_2PO_3H_2$ and $PdCl_4^{2-}$. The hydrothermal system gives materials in which the $PdCl_4^{2-}$ ions are homogeneously distributed throughout the volume of the catalyst and could be reduced by hydrogen to obtain nanoaggregates (based on TEM analysis). Unfortunately, we observe a decrease in crystallinity of the sample due to the large size of $PdCl_4^{2-}$ ions, relative to the Cl^- ions of the nonmetalated HfPOPV(X).

From TEM micrographs (Fig. 1) and XRD (Fig. 2), it is clear that the ion-exchanged/reduced catalysts are significantly more crystalline than the hydrothermal catalysts. The crystal sizes of the ion-exchanged/reduced catalyst are larger than those made from hydrothermal incorporation. Figure 1 also shows the differences in particle size of $Pd^{(0)}$ in both catalysts and conclusively demonstrates that the hydrothermally incorporated catalyst has much better metal dispersion than the ion-exchanged one. As described in our previous work (14), both ion-exchanged and reduced catalysts were analyzed using Pd K-edge X-ray absorption spectroscopy (XAFS). The oxidation state of palladium in the ion-exchanged sample was confirmed to be 2+. It was found to be coordinated with 4 Cl^- ions in square planar geometry. Upon reduction with hydrogen, XAFS analysis clearly revealed the formation of Pd nanoaggregates having the oxidation state of 0. XAFS calculations for the ion-exchanged and reduced catalyst showed the average size of Pd to be about 17 Å, although TEM micrographs show several larger aggregates of sizes 45–50 Å. This showed that, in the ion-exchanged/reduced catalyst, very poor control in particle size was achieved, leading to a wide Pd-particle size distribution.

ICP-MS has been used to determine the overall Pd loading and the Pd to P ratios; the results are listed in Table 1. The quantity of P in the material can be used as an indicator of the loading of viologen in the material, as the ratio of P to viologen is 3 : 1 in HfPOPV(X). If the ratio of Pd : viologen is 1 : 1, the ratio of Pd : P would be 1 : 3. The Pd : P ratio determined for these samples vary from 1 : 3.6 to 1 : 5, close to that expected for a 1 : 1 ratio of Pd to viologen.

Nonaqueous Reaction Media for H_2O_2 Production

The catalytic reactions carried out here were run at atmospheric pressure and room temperature in open plastic tubes. The catalyst and reaction medium were stirred magnetically, while separate H_2 an O_2 gas streams were

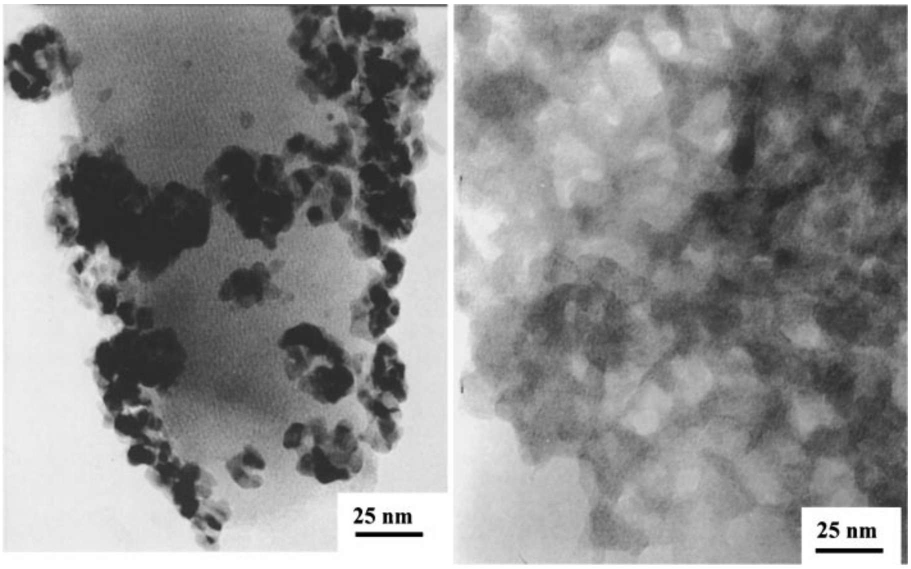

FIG. 1. Comparison of ion-exchanged (left) and hydrothermally incorporated (right) catalysts synthesized in the presence of a high concentration of HF.

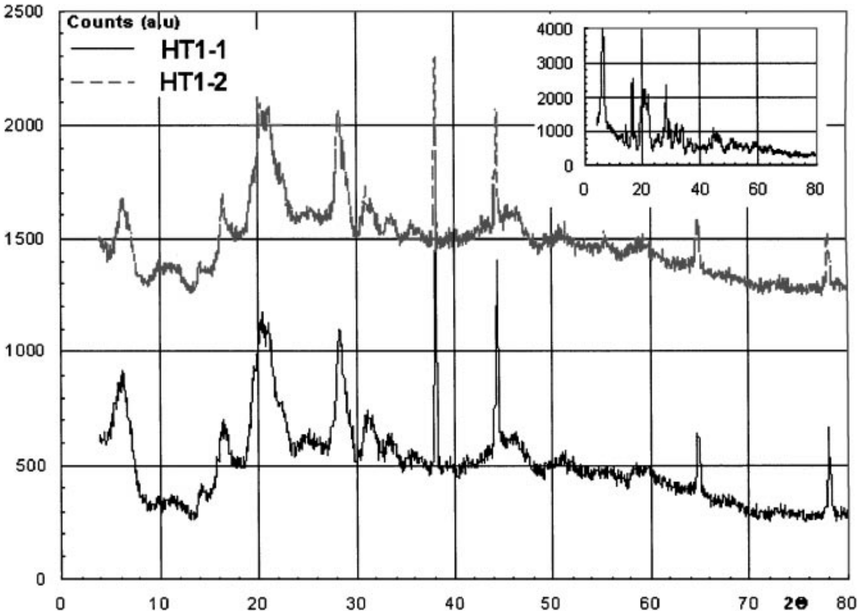

FIG. 2. XRD pattern obtained from two catalysts synthesized in the presence of PdCl$_4^{2-}$: HT1-1 (low HF concentration) and HT1-2 (high HF concentration). The inset shows an XRD pattern of the HfPOPV structure, low HF concentration.

bubbled through the suspension. The flow rates for H_2 and O_2 were controlled with mass flow controllers and their ratio kept below the explosive limit, i.e., less than 5% H_2. The buildup of H_2O_2 has been investigated using several catalysts and different reaction media. The catalysts used in this paper include those prepared by ion exchange and by hydrothermal incorporation of Pd. The reaction media investigated included a number of different organic solvents, which were made acidic with dilute H_2SO_4 or HCl. Figure 3 shows the rate of hydrogen peroxide production in a reaction medium consisting of 10 ml of 0.1 M aqueous H_2SO_4 and 20 ml of a given organic solvent. Methanol, ethanol, isopropanol, acetone, and dioxane were examined, along with pure water as a reference. The catalyst (25 mg) used in this sequence of experiments was IEx (prepared by ion exchange and reduction). The methanolic medium showed 200 mM production of hydrogen peroxide, after 6 h, while isopropanol and ethanol solvents give 175 and 160 mM, respectively, in the same time. The acetone–sulfuric acid mixture gave 200 mM H_2O_2 in 6 h. The dioxane–sulfuric acid media gave 125 mM in 6 h. The water–sulfuric acid mixture gave less than 5 mM H_2O_2 in the same time. We estimate the error bars in these measurements as ±20 mM. The errors arose due to two factors—sampling and reproducibility. The error in reproducibility is larger and was estimated by running several parallel experiments with the same catalyst and conditions, observing deviations in $[H_2O_2]$ buildup from run to run. The acetone and alcohol systems are clearly better than the dioxane system. The fact that the aqueous system was ineffective is consistent with our previous report (13). Production of H_2O_2 with the catalysts studied here was only observed when HCl or HBr was used, leading to a strong "halide effect" (13). Experiments were carried out with both HCl and H_2SO_4 in organic media to determine if this halide effect is observed in organic media. Figure 4 shows the performance of the best organic media with both HCl and with H_2SO_4. The presence or absence of halide ion does not have a significant effect on H_2O_2 production in organic solvents, as shown

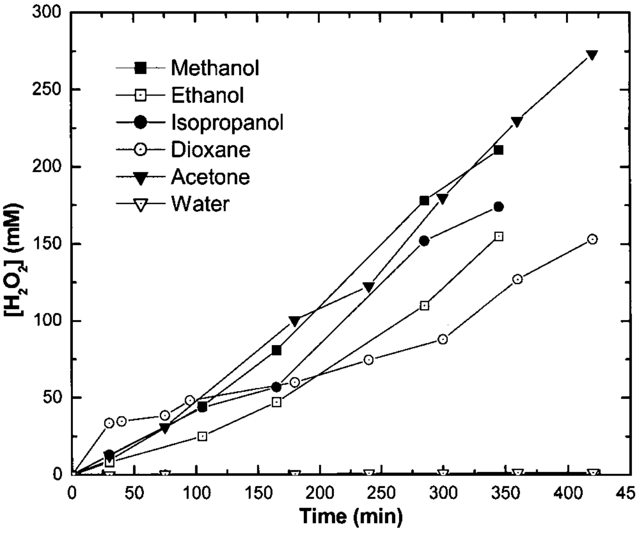

FIG. 3. Comparison of different reaction media used with sulfuric acid: 10 ml of 0.1 M H_2SO_4/20 ml of organic solvents or water. Acetone and methanol appear to be the best organic media. Dioxane is poorer than either.

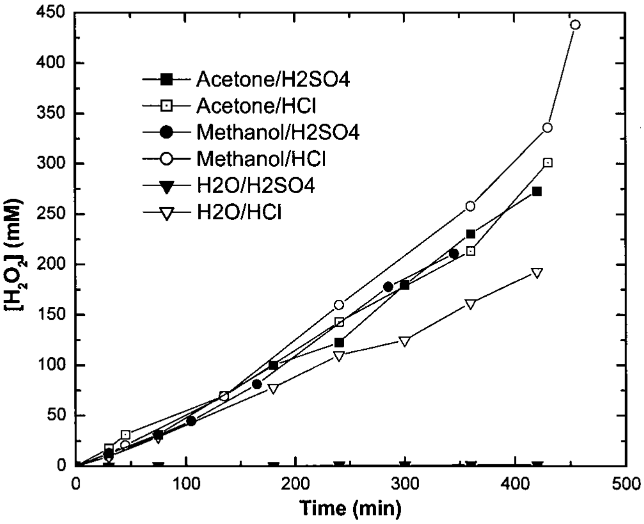

FIG. 4. Evaluation of the best suitable organic media: methanol and acetone to explore the effect of H_2SO_4 instead of HCl. Catalyst: IEx. No effect of halide at all in methanol or in acetone, whereas aqueous H_2SO_4 (unlike aqueous HCl) does not produce any significant amount of hydrogen peroxide.

for acetone and methanol in Fig. 4. We cannot completely rule out chloride ion being required at trace levels, however, since small amounts of Cl^- ion are present in the catalyst. A strong halide effect has been reported for supported metal catalysts as well, which require mM levels of Cl^- or Br^- promoter/cocatalysts for efficient H_2O_2 production (2–4).

To determine if water in the organic solvent plays a role in catalysis, the reaction was carried out with anhydrous methanol, acidified with concentrated acid. For this experiment the reaction medium consisted of 30 ml of anhydrous methanol and 51 μl of concentrated sulfuric acid. A second reaction was run in parallel, which used 30 ml of MeOH/H_2O at a 2/1 ratio. The $[H^+]$ for both of these reactions was 0.023 M, which was the same concentration of H^+ used in the previous catalysis runs. Catalyst HT3 (25 mg) was used for this reaction. The anhydrous MeOH system gave significantly higher rates of H_2O_2 production than the aqueous MeOH system. The anhydrous system gave 3 M H_2O_2 after 20 h, while the MeOH/H_2O system produced only 1 M H_2O_2 over the same time. Increasing the amount of catalysts used in the reaction from 25 to 100 mg, while keeping the volume of the medium constant, did not affect the rate of H_2O_2 production.

To compare the two different types of catalyst, two parallel reactions were carried out with ion-exchanged/reduced and hydrothermally incorporated catalysts, using acetone/H_2SO_4 as the reaction medium. The same total weight of catalyst, 25 mg, was used in each reaction. The results are shown in Fig. 5. The rate of buildup of H_2O_2 with time is very similar in both catalysts, despite the fact that the loading of Pd in the ion-exchanged/reduced catalyst (IEx) is 11.5% by weight, whereas it is 5.7% by weight in the case of the hydrothermally incorporated (HT1) catalyst. From TEM micrographs, it is clear that the dispersion of $Pd^{(0)}$ in the case of the hydrothermally incorporated catalyst is much higher than that of the ion-exchanged/reduced catalyst. TEM micrographs (Fig. 1) show Pd particles of 20 Å or less in the case of HT1 as compared to 50 Å in the case of IEx. There is no evidence of any enhancement of net rate of H_2O_2 production due to this improved dispersion. The hydrothermally incorporated catalysts are very stable under our reaction conditions. HT2 gives over 3.5 M H_2O_2 after 45 h (MeOH/H_2O medium, 33% H_2O, 0.03 M H_2SO_4, with 25 mg of catalyst). A significant advantage of the hydrothermal route is the preparation of the catalyst, a one-step process, which is much simpler than the ion-exchanged route and requires smaller quantities of $PdCl_4^{2-}$.

Selectivity for Hydrogen Peroxide Production

The production of H_2O_2 from O_2 competes with its depletion by further reduction of H_2O_2 to water, i.e., $H_2 + H_2O_2 \rightarrow 2H_2O$. To determine the selectivity for O_2 reduction over H_2O_2, we have measured the concentration of both H_2O_2 and H_2O throughout the course of the reaction, using anhydrous MeOH as the initial reaction medium (Fig. 6). This selectivity is equivalent to the percentage yield of H_2O_2 based on H_2 consumed. The $[H_2O_2]$ was determined colorimetrically and the $[H_2O]$ by gas chromatography, GC. Unfortunately, the H_2O_2 decomposes on the GC column, giving a water signal, which interferes with the water measurement. The GC measurement can be easily corrected for the H_2O_2 contribution to the H_2O signal since the $[H_2O_2]$ was independently measured. To eliminate

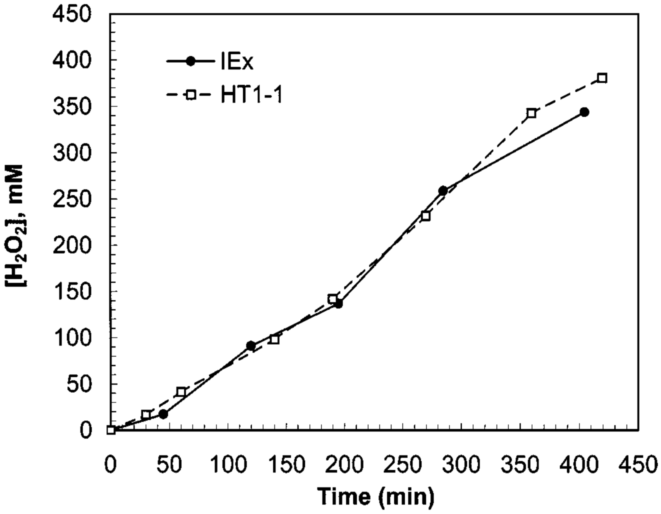

FIG. 5. Comparison of two catalysts: IEx, ion exchanged and reduced, with large crystals and Pd particle sizes of about 40–50 Å and Pd loading of 11.5% by weight versus HT1-1, hydrothermally incorporated Pd, with 5.7% by weight Pd loading and particle size of about 15–20 Å. No difference at all in H_2O_2 buildup rates.

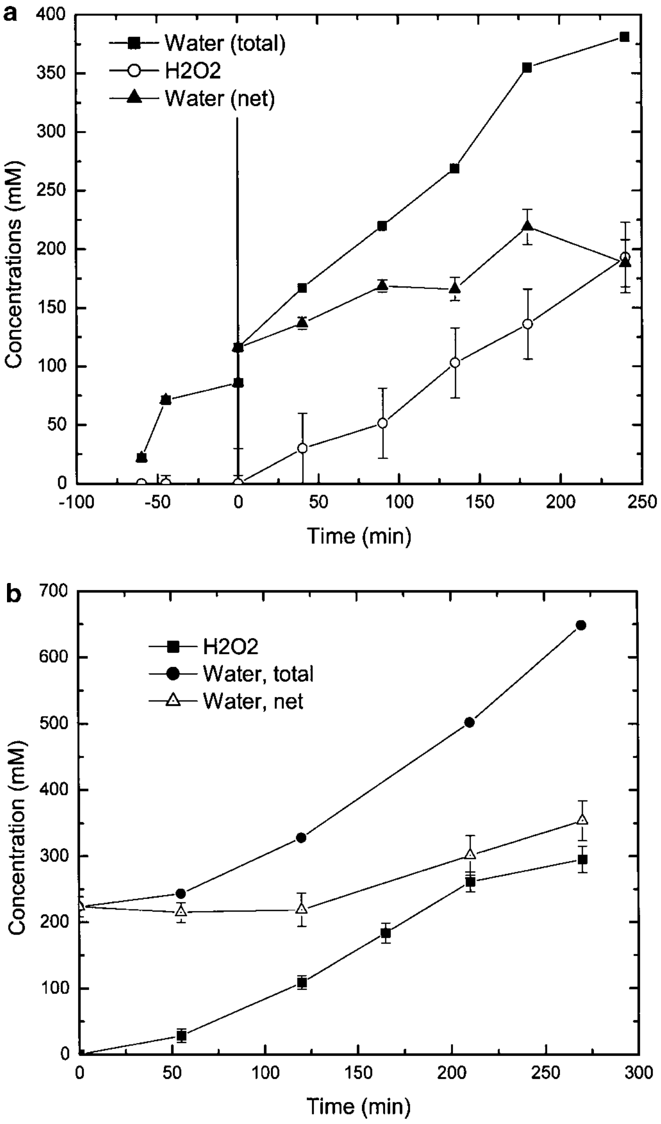

FIG. 6. (a) Catalyst HT1-1: The buildup of H_2O_2 and water as well with time. Selectivity toward $H_2O_2 = 82\%$. (b) Catalyst HT3-2 (selectivity = 74%): Buildup of water prior to the start of the reaction. Sources of water include catalyst, prereducing the catalyst, and MnO_2 used for the decomposition of H_2O_2. Observe the sudden jump in the water level when a sample is measured at time = 0, with 1–2 mg of MnO_2. Commercial MnO_2 contributes about 28 mmol of water when 1–2 mg is used for 0.2 ml of sample is withdrawn. For $t \leq 0$ "Water(total)" and "Water(net)" symbols overlap.

errors that would result from incomplete decomposition of H_2O_2 on the GC column, all samples were treated with MnO_2 prior to GC analysis to completely decompose the H_2O_2 (by autoxidation). An initial water signal in these plots is observed, resulting from the catalyst prereduction step, either directly from H_2 reduction step itself or from water that had been bound to the catalyst. The water from the prereduction process is shown building up in the negative time part of Fig. 6a. A second contribution to the water signal is observed at time 0 in this plot. This is due to the water absorbed onto the MnO_2, used to decompose the H_2O_2 prior to GC analysis. Both the prereduction and MnO_2 decomposition steps lead to a consistent background level of water that is not related to the catalysis. The "net" concentration of water is determined by subtracting the total water accumulated up to time = 0 from the observed GC measurement. The selectivity for the H_2O_2 catalysis have been calculated using Eq. [2]. Catalyst HT3-2 gives an average selectivity of 74% toward H_2O_2 and HT1-1 shows 82% selectivity over the first 4 h of reaction.

DISCUSSION

In our previous investigations it was shown that the presence of halide ions is crucial to the H_2O_2 production process using a MPOPV(X) · Pd catalyst in aqueous media (13). When the HCl used to acidify the aqueous reaction medium was replaced with H_2SO_4, very low levels of H_2O_2 were observed. Numerous patents (1–7) published in the field of direct production of H_2O_2 (mostly supported Pd catalysts) indicate the importance of halides either in the reaction media or in the catalyst (fluorinated supports) (6). Chuang and Zhou (6) proposed that the role of halide was to tune the surface properties of the catalyst. The interaction of the reaction medium with the surface of the catalyst is very important. The balance between hydrophilicity and hydrophobicity of the support and the reaction medium appears to be an essential factor, as it determines the desorption of H_2O_2 from the surface into solution. An extremely hydrophobic support would limit the interaction of dissolved gases with the solid whereas an extremely hydrophilic support would prevent desorption of H_2O_2 from the surface (6). In our system, halide ions are not necessary when the reaction medium is an organic solvent. In fact, acetone and alcohols give significantly higher rates of production of H_2O_2 in the presence of sulfuric acid than aqueous HCl. It is not clear whether the hydrophobic/hydrophilic nature of the catalyst in the presence of different media is responsible for this behavior or not. However, the difference in the rate of production may be attributed to external mass transfer control and solubility, as discussed below.

In any heterogeneous catalytic reaction, an external mass transfer resistance will exist. In a three-phase slurry reactor system, the reaction medium could control both mass transfer resistances, i.e., gas–liquid film resistance and dissolved gas–solid film resistance. The gas–liquid mass transfer rate would therefore depend upon the interfacial velocity of the gas bubbles, i.e., on the rate at which they rise to the surface and on the transport properties of the liquid medium (viscosity, diffusivity of H_2, and density) (15). The flow rate of oxygen through the liquid is at least 10 times higher than that of hydrogen. Thus, the most significant mass transfer resistance should be for hydrogen at the gas–liquid interface and not for oxygen at this interface. The mass transfer rate equation is given in Eq. [3] (15–17), where $k_{\mathrm{l-g}}$ is the mass transfer coefficient, $a_{\mathrm{l-g}}$ is the interfacial area of the bubble–liquid interface throughout the volume of the liquid, $C_{\mathrm{l-g}}$ is the dissolved gas concentration at the gas–liquid interface, mol/cm^3, and C_{l} is the dissolved gas concentration in the liquid bulk, mol/cm^3:

$$\text{Gas–liquid mass transfer rate} = k_{\mathrm{l-g}} a_{\mathrm{l-g}} (C_{\mathrm{l-g}} - C_{\mathrm{l}}). \quad [3]$$

The mass transfer coefficient ($k_{\mathrm{l-g}}$) at the liquid–gas interface can be estimated as follows. A semiempirical correlation of the Sherwood number (Sh) with the Rayleigh number (R_{a}) has been discussed by Treybal and is shown in Eq. [4] (16). Sherwood number is a dimensionless number, reflecting the ratio of mass transport by convection to transport by diffusion. The Rayleigh number is a measure of the forced convection due to bubbling a gas in a liquid and can be calculated as shown in Eq. [5]. Here, d_{b} is the diameter of the bubble, approximately 0.3 cm (estimated by visual observations), $\Delta\rho$ is the difference in density between the liquid media (ρ_{l}) and the gas (ρ_{g}), μ_{l} is the viscosity of liquid media (poise), g is acceleration due to gravity (981 cm/s^2), and D_{l} is the diffusivity of gas in a liquid (in cm^2/s). Treybal's expression can be readily solved for $k_{\mathrm{l-g}}$, the liquid film mass transfer coefficient at the liquid–gas interface, by considering the system to involve only a vertical rise of gas bubbles through a column of liquid and minimal agitation. Our conditions are similar, as the agitation is only at the base. The tubes bringing the gases are approximately 1 cm above the stirrer. Although the liquid is agitated, the rise of bubbles is essentially vertical:

$$\mathrm{Sh} = k_{\mathrm{l-g}} d_{\mathrm{b}} / D_{\mathrm{l}} = 2.0 + 0.31 (R_{\mathrm{a}})^{1/3} \quad [4]$$

$$R_{\mathrm{a}} = \left(d_{\mathrm{b}}^3 \Delta\rho g\right) / (D_{\mathrm{l}} \mu_{\mathrm{l}}). \quad [5]$$

The size of the bubble is a function of the surface tension at the liquid–gas interface and the hydrostatic pressure. But here, we have assumed simplistically that d_{b} is constant at approximately 0.3 cm, slightly larger than the outer diameter of the delivery tube. The estimation of diffusivity, D_{l}, is carried out using the semiempirical method developed by Wilke–Chang (17) and is subject to a 5–10% error. It is 4.5×10^{-3} cm^2/s for methanol and 2.4×10^{-3} cm^2/s for water at room temperature. The viscosity of methanol is 0.54 cp and is 0.89 cp for water at room temperature. Using the above formula (Eqs. [4] and [5]) gives mass transfer coefficients for the hydrogen–methanol system of 0.467 cm/s and a value of 0.28 cm/s for the hydrogen–water system.

To estimate the mass transfer rate of hydrogen into solution (Eq. [3]), the interfacial area ($a_{\mathrm{l-g}}$) of the gas in the liquid media must be estimated. If the bubble rises through a length, L, of liquid, the residence time, $t_{\mathrm{r}} = L/u_\infty$, where u_∞ is the rise velocity (the terminal velocity of a sphere) which may be calculated by a force balance of the buoyant force on the bubble and the drag force on it (18). Multiplying the residence time (t_{r}) with the flow rate of gas will give us the gas volume hold-up in the liquid. The gas hold-up calculated this way might be multiplied by the average surface to volume ratio of a bubble ($6/d_{\mathrm{b}}$), thereby yielding the total liquid–gas interfacial area ($a_{\mathrm{l-g}}$). For the H_2–methanol system, the area is 0.71 cm^2 and for H_2–water it is 0.38 cm^2. The term $k_{\mathrm{l-g}} a_{\mathrm{l-g}}$ for the H_2–methanol system is 0.33 cm^3/s and for the H_2–water system it is about 0.11 cm^3/s; i.e., $k_{\mathrm{l-g}} a_{\mathrm{l-g}}$ for H_2–methanol is about 3 times that for H_2–water.

TABLE 2

Solubility of Hydrogen and Oxygen in Various Organic Solvents at Room Temperature (19, 20)

Solvent	Solubility H_2, mg/L (mM)	Solubility O_2, mg/L (mM)
Methanol	7.91 (3.96)	324 (10.12)
Ethanol	7.50 (3.75)	320 (10.0)
Isopropanol	6.92 (3.46)	323 (10.1)
Acetone	8.15 (4.08)	364 (11.38)
Water	1.62 (0.81)	40 (1.25)
1,4-Dioxane	4.12 (2.06)	231 (7.22)

In addition to the role of the mass transfer coefficients in determining the rate of reaction, the dissolved gas concentration in the medium is also important. The solubilities of oxygen and hydrogen in several solvents are given in Table 2. The rate of mass transfer of H_2 may be calculated from Eq. [3]. If we assume that the rate of consumption of hydrogen is fast, $C_{\mathrm{l}} \approx 0$. In the case of methanol, the rate of mass transfer of $H_2 = 0.079$ mmol/min and in water the rate $= 0.0053$ mmol/min. The rate of mass transfer in methanol is almost 15 times that of water, according to this calculation, primarily because the solubility of H_2 in methanol is much higher than that in water. While a clear-cut comparison of H_2O and methanol media cannot be made due to the observed halide effect in water, our calculations support the significant rate enhancement in organic solvents relative to water.

Support of the limitation being mass transfer at the liquid–gas interface comes from two observations. The first is that anhydrous media give higher rates of H_2O_2 production than mixed water–alcohol mixtures. Both HCl and H_2SO_4 work equally well, so a halide effect is not present in either anhydrous or mixed systems. If no water is present in the system, the liquid film mass transfer coefficient is enhanced and the rate of peroxide production increased. The second observation that supports a mass transfer limitation is the fact that increasing the amount of catalyst present by a factor of 4, while keeping the quantity of the reaction medium constant, did not affect the rate of H_2O_2 build-up. The rate of H_2O_2 formation is therefore not the intrinsic kinetic rate of reaction.

Liquid–solid interfacial transport is the slowest when particles are suspended in stagnant liquid. The Sherwood number for liquid–solid mass transport under these conditions would be roughly equal to 2 (17). With a mean d_p (particle diameter) of about 100 μm, the $k_{l\text{–}s}$ for the H_2–methanol system is approximately 0.89 cm/s and for H_2–water it is about 0.48 cm/s. Estimating the solid–liquid interfacial area, $a_{l\text{–}s}$, by the formula $a_{l\text{–}s} = (6/d_p)V_s$, where V_s is the volume of the solid phase, we will obtain $k_{l\text{–}s}a_{l\text{–}s} = 9.6$ cm^3/s for methanol and 5.1 cm^3/s for water. A comparison of these numbers with the $k_{l\text{–}g}a_{l\text{–}g}$ for H_2–methanol (0.33 cm^3/s) and H_2–water (0.11 cm^3/s) reveals clearly that even in the worst possible liquid–solid contact situation, the resistance to mass transfer across the solid–liquid interface is much lower than that across the liquid–gas interface $(1/(k_{l\text{–}s}a_{l\text{–}s}) \ll 1/(k_{l\text{–}g}a_{l\text{–}g}))$.

CONCLUSIONS

The rate of production of H_2O_2 from H_2 and O_2 with HfPOPV(X)·Pd catalysts is strongly influenced by the choice of solvent used for the reaction medium. Reaction media consisting of sulfuric acid in an organic solvent (acetone, alcohols, and dioxane) give good yields of H_2O_2, whereas aqueous sulfuric acid shows very low levels of activity. We attribute the large difference between water and organic solvents to the liquid film mass transfer at the gas–liquid interface being rate determining. To verify this hypothesis, film coefficients at the liquid–gas interface have been estimated using semiempirical models for the hydrogen–methanol interface and the hydrogen–water interface. Coupled with the gas solubility of H_2 in methanol and in water, the rate of mass transfer of H_2 across the gas–liquid interface for the methanol system is calculated to be almost 15 times that of water (0.08 and 0.0053 mmol/min, respectively). This calculation lends support to the hypothesis that liquid film mass transfer at the gas–liquid interface is the rate-determining step in the production of H_2O_2 in sulfate-containing media.

In organic media, similar results are obtained if HCl is used in place of H_2SO_4. In aqueous media, however, the switch from sulfuric to hydrochloric acid makes a significant difference. While aqueous H_2SO_4 gives little or no H_2O_2 under the conditions used here, aqueous HCl is a more effective reaction medium than acidic dioxane and comparable to acidic isopropanol ($[H_2SO_4] = 0.03$ M). Similar halide dependence has been reported for supported metal catalysts (2, 3, 4, 6), which require a halide activator or co-catalysts. A possible explanation for the halide dependence observed for HfPOPV(X)·Pd catalysts in aqueous media is that the Pd particles may be the active sites in aqueous media and the reduced viologen sites in organic media. The viologen sites would not be expected to show an acid (halide) dependence, while catalysis at the supported metal particles has been shown to give strong halide dependence. The observation that the catalyst produces H_2O_2 continuously over 45–50 h (1 atm H_2 and O_2), without stabilizers or additives in the reaction media, suggests that the catalyst does not lose activity over time. Since the rate of H_2O_2 production is limited by mass transfer, however, we cannot rule out some (not complete) loss of catalyst activity during the course of the experiment.

The selectivity toward H_2O_2 production for some of these hydrothermally incorporated catalysts is over 80%, which is very encouraging. Another important feature is the ease of synthesis of hydrothermally incorporated catalyst. Current efforts are directed toward enhancing liquid–gas mass transfer to arrive at a regime where the measured rates reflect the intrinsic activity of the catalyst toward hydrogen peroxide production.

REFERENCES

1. "Encyclopedia of Chemical Technology" (Kirk and Othmer, Eds.), Vol. 13. Wiley, New York, 1996.
2. Gosser, L. W., and Schwartz, J. T., U.S. Patent 4832938, 1989.
3. Gosser, L. W., and Schwartz, J. T., U.S. Patent 4772458, 1988.
4. Gosser, L. W., and Paoli, M. A., U.S. Patent 5135731, 1992.
5. Kawakami, M., Ishiuchi, Y., Nagashima, H., Tomita, T., and Hiramatsu, Y., U.S. Patent 5399334, 1995.
6. Chuang, K. T., and Zhou, B., U.S. Patent 5338531, 1994.
7. Dalton, A. I., Jr., Greskovich, E. J., and Skinner, R. W., U.S. Patent 4389390, 1983.
8. Meiers, R., and Holderich, W. F., *Catal. Lett.* **59**(2–4), 161 (1999); Meiers, R., Dingerdissen, U., and Holderich, W. F., *J. Catal.* **176**, 376 (1998).
9. Farrington, J. A., Ebert, M., Land, E. J., and Fletcher, K., *Biochem. Biophys. Acta* **372**, 314 (1973).
10. Vermeulen, L. A., Snover, J. L., Sapochak, L. S., and Thompson, M. E., *J. Am. Chem. Soc.* **115**, 11767 (1993); Vermeulen, L. A., and Thompson, M. E., *Chem. Mater.* **6**, 77 (1994).
11. Byrd, H., Clearfield, A., Poojary, D., Reis, K. P., and Thompson, M. E., *Chem. Mater.* **8**(9), 2239 (1996).
12. Miller, D. S., Bard, A. J., McLendon, G., and Ferguson, J. J., *J. Am. Chem. Soc.* **103**, 5336 (1981).
13. Reis, K. P., Joshi, V. K., and Thompson, M. E., *J. Catal.* **161**, 62 (1996).
14. Dokoutchaev, A., Krishnan, V. V., Thompson, M. E., and Balasubramanian, M., *J. Mol. Struc.* **469**, 191 (1998).
15. Shah, Y. T., "Gas-Liquid-Solid Reactor Design." McGraw-Hill, New York, 1979.
16. Treybal, R. E., "Mass Transfer Operations." McGraw-Hill, New York, 1980.
17. Bird, R. B., Stewart, W. E., and Lightfoot, E., "Transport Phenomena." Wiley, New York, 1960.
18. McCabe, W. L., Smith, J. C., and Harriot, P., "Unit Operations of Chemical Engineering." McGraw-Hill, New York, 1985.
19. Fogg, P. G. T., and Gerrard, W., "Solubility of Gases in Liquids." Wiley, New York, 1991.
20. Luhring, P., and Schumpe, A., *J. Chem. Eng. Data* **34**, 250 (1989).